Adaptive dung beetle optimization-based agile perturb and observe technique for energy management system

Shweta Sengar, Aniket Kumar
School of Electronics, Electrical and Mechanical Engineering, Shobhit Institute of Engineering and Technology (Deemed to be University), Meerut, India

Article Info

ABSTRACT

Energy storage system (ESS) plays a significant role in maximizing the use of renewable energies to ensure a balance between power generation and demand. ESS assists in maintaining grid stability by providing backup power during fluctuations or outages and smoothing out the variability of renewable energy source (RES). However, EMS fails to effectively balance dynamic interactions due to the unpredictable nature of renewable energy sources (RES) which results in a suboptimal performance. This research proposes an adaptive T-distribution dung beetle optimization-based agile perturb and observe technique (ADBO-APO) for EMS. Photovoltaic (PV) module, battery, and wind turbine are the three sources utilized to establish an effective EMS in a grid-connected system. The ADBO is applied to manage the switching between battery storage and wind turbines. The APO is utilized for triggering the bidirectional DC-DC switch to obtain stable power from wind, PV, and battery. APO enhances EMS by involving perturbation levels for optimal power extraction. It improves the stability and efficiency across variable energy sources. The proposed ADBO-APO achieves a superior average index of 1.2598×104 when compared to the existing method, levy flight quasi oppositional based learning smell agent optimization (LFQOBL-SAO).

Corresponding Author:

Shweta Sengar
School of Electronics, Electrical and Mechanical Engineering
Shobhit Institute of Engineering and Technology (Deemed to be University)
Meerut, Uttar Pradesh, India
Email: shwetasengar17@gmail.com

1. INTRODUCTION

Renewable energy source (RES) plays a significant role in power production due to their clean and environment-friendly nature. Because of its high dependence on climate and weather conditions in various cases, the finest possible system is the renewable energy hybrid system with energy storage systems (ESS) [1], [2]. Photovoltaic (PV), wind turbines, and battery are considered the primary favorable RES because they generate a huge infinite amount of clean energy [3], [4]. PV solar energy is one of the most widely employed technologies with approximately 1 Terawatt (TW) of power capacity worldwide. The rapid solar cell development and cost reduction have contributed to a rise in grid-connected PV power systems [5], [6]. The front-end phase direct current/direct current (DC/DC) is adapted for optimizing the potential of PV cells in power variation which enhances the efficiency [7], [8]. The PV system produces DC and requires an inverter to generate power for the grid [9], [10]. The microgrid (MG) is established to combine ESSs and distributed energy resources (DERs) in a controlled and safe way [11], [12]. The battery EES (BEES) is a primary reliable EES utilized in the market, possessing abilities for development in various applications of renewable energy [13], [14]. Moving power point tracking (MPPT) is used for tracking maximum power points with

subsequent changes in temperature or radiation [15], [16]. Hybrid systems provide numerous advantages to enhance rural energy access reliability, dispatchable renewable energy, minimize long-term energy costs, enhance the eco-efficiency of energy production, and decrease the dependence on fossil fuels [17]. Also, it presents modern energy access to remote areas without the requirement of distribution lines and expensive transmission from the central grid [18], [19]. Nevertheless, EMS struggles to effectively balance dynamic interactions because of the unpredictable nature of RES which results in suboptimal performance. Babu *et al.* [20] suggested a multi-objective optimization by utilizing a genetic algorithm for an EMS. The system of energy storage was comprised of an MG network significant for smooth power transfer and effective energy management. The suggested approach utilized long-short-term memory (LSTM) to predict PV and wind generation values which help in determining an optimal value for grid power and battery usage. However, the genetic algorithm was trapped in local optima because it depended on evolving the solutions through a process of selection, mutation, and crossover which did not adequately explore the entire search space.

Mas'ud *et al.* [21] presented a levy flight quasi oppositional based learning smell agent optimization (LFQOBL-SAO) for PV, battery, and wind systems. An initial solution was generated randomly for hybrid systems decision variables which allocated an initial velocity to every solution. The fitness of this mode was determined and the molecules with optimal nominee solution were selected as the agent. Nevertheless, LFQOBL-SAO based on historical data and predefined flight patterns limited its ability to quickly adjust to the new or fluctuating conditions which minimized the effectiveness in dynamic environments. Boualem *et al.* [22] implemented an Elman neural network (ENN) for a grid-connected PV-wind battery system. The state flow (SF) was used for EMS to extract the testing and training data for the ENN construction controller. The rule-based SF reduced the linguistic rules' complexity in intricate scenarios with fewer execution times which in turn assured and increased the smart switch among various operation modes. Nonetheless, the SF struggled with limited generalization when extracting testing and training data for ENN because it was based on predefined state transitions and deterministic rules.

Azaroual *et al.* [23] developed a model predictive control (MPC) for EMS in PV, wind, and battery. The developed approach was a closed-loop control to variations of RES and prevented battery systems from passing into deep discharge. The MPC enhanced the overall system index performance by minimizing the amount of energy which avoided the deep battery drain. Nevertheless, MPC faced struggles with the integration and coordination of multiple energy sources because of the difficulty in predicting and modeling dynamic interactions among different sources which led to mismatches between demand and supply. Ullah *et al.* [24] introduced a hybrid of four control techniques based on fuzzy logic, artificial neural network (ANN), proportional integral derivative, and sliding mode controller (SMC) for EMS. The solar power maximization issue was solved by utilizing MPPT in an ANN approach. Nonetheless, the hybrid approach faced challenges in achieving seamless integration and coordination between different control strategies because of the use of different mechanisms in each control strategy which resulted in inefficiencies. In the overall analysis, the existing methods are seen to have the following limitations: getting stuck in the local optima, struggling to adapt to new or fluctuating conditions, and difficulty in predicting and modeling the dynamic interactions. In order to solve these issues, the ADBO-APO is proposed by using three sources which include the battery storage system, PV, and wind turbine for EMS which facilitated an improved overall energy management and stability.

The major contributions of this research are explained as follows:
- In traditional DBO, a T-distribution is added to enhance the convergence speed during the dung beetles foraging stage. ADBO effectively balances energy sources by dynamically adjusting to the changing conditions which ensures optimal switching between PV, wind, and battery storage systems.
- The APO enhances EMS by involving perturbation levels for optimal power extraction which improves the stability and efficiency across variable energy sources.
- In EMS, a bidirectional DC-DC converter is used to enable an effective energy flow in both directions and allows storage and energy retrieval among the source and storage devices.

The remaining portion is structured as: Section 2 explains the proposed method, while section 3 illustrates an adaptive T-distribution dung beetle optimization, section 4 provides results and discussion for the existing methods and the proposed method, and finally, the conclusion is given in section 5.

2. PROPOSED METHOD

In this research, ADBO-APO is proposed for EMS which contains two RES of PV and wind turbine, and 1 storage system of battery. A bidirectional DC-DC converter is used to allow for an effective energy flow in both directions. An adaptive t-distribution is used to balance exploitation and exploration which increases convergence speed. Figure 1 shows a block diagram for the proposed method.
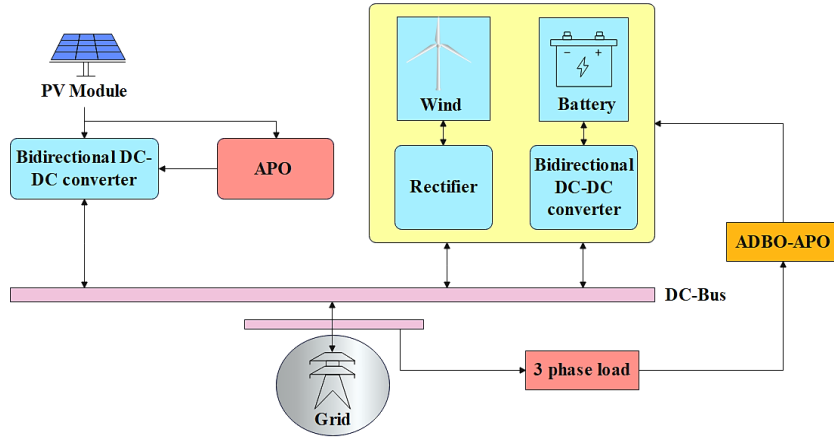
Figure 1. Block diagram for the proposed method

2.1. Modeling of microgrid

An MG is the distributed energy resources and interconnection of loads that function as a single entity associated with a grid. Power converters are significant in MG to integrate renewables into the traditional power systems. Energy storage such as a battery is linked to a DC bus via a bidirectional DC-DC converter. The description of the PV module, wind turbine, and battery are explained in the following sub-sections.

2.1.1. PV module

A PV [20] module is a primary component in EMS that converts sunlight into electrical energy by utilizing solar cells. The power of PV generation differs because of the meteorological variables of temperature and solar irradiation. A solar PV power output is estimated using (1) where $P_{pv}(t)$ and $C_{pv}(t)$ represents PV's output power and rated capacity in kW, $S_t(t)$ and S_{std} indicate solar irradiance at PV panels ($\frac{kW}{m^2}$), and η^{PV} denotes the converter efficiency.

$$P_{pv}(t) = C_{pv} * \left(\frac{S_t(t)}{S_{std}}\right) * \eta_{loss}(t) * \eta_{DC/DC}^{PV} \tag{1}$$

2.1.2. Wind turbine

In an EMS, a wind turbine [20] converts kinetic energy from the wind into electrical power. It assists in integrating renewable energy sources which optimize energy production and consumption. In a wind turbine, the extracted amount of energy is detected by turbine parameters and the speed of wind which is calculated in (2) where, C_p indicates the wind turbine's power coefficient, r represents a radius of wind turbine blades, and V determines the wind speed.

$$P_{W(t)} = \frac{1}{2}\rho C_p V_\omega^3 \pi r^2 \tag{2}$$

2.1.3. Battery

In an EMS, a battery [20] stores electrical energy for later use which provides backup power and balances demand and supply. It helps optimize energy usage and increase the system's efficiency and reliability. The battery is exhibited as an equivalent circuit with a voltage source E_{bat} in series by an internal resistance R_{bat} which is represented in (3).

$$V_{bat} = E_{bat} - R_{bat}.I_{bat} \tag{3}$$

Where, E_{bat} denotes the internal voltage (V), V_{bat} represents terminal voltage (V), and R_{bat} determines internal resistance (Ω). The battery's state of charge (SOC) is computed in (4). The $SOC(t_0)$ and C_N represents the initial battery SOC (%) and the battery's nominal capacity (Ah). Table 1 displays the components of RES with their specifications.

$$SOC(t) = SOC(t_0) = \frac{1}{C_N}\int_0^1 i_{bat}(t)dt \tag{4}$$

Table 1. Components of RES with their specification

Components	Parameters	Specifications
PV	Nominal power	300 W
	Open circuit voltage	5.68 A
	Maximum power current	5.68 A
	Short-circuit current	6.05 A
	Maximum power voltage	49.58 V
Wind turbine	Stator resistance	5.7 $m\Omega$
	Inductance armature	0.14
	Number of poles	4
	Inertia	0.0000003
Battery	Nominal capacity	2.4 kWh
	Battery depth of discharge	0.8
	Model	Lead acid
	Nominal voltage	12 V

2.2. Modeling of bidirectional DC-DC converter

It is an EMS that allows for effective energy flow in both directions which enables the storage and energy retrieval among the source and storage devices. This capability supports dynamic energy balancing which increases flexibility and optimizes the usage of RES. A trial sustainable power test source contains 3 significant portions: RES (wind turbine and PV), comprising battery and super-capacitor-based ESS (SC-ESS), load, and appropriate power electronics converters. A switch over the SC, PV, and battery are $C1, C2, P1, B1$, and $B2$ used to activate the buck-boost process. The switches turn ON and OFF are used according to load and power transfer availability. To activate the unidirectional current flow, the $D_{S1}, D_{S2}, D_{B1}, D_{B2}$, and D_{P1} are switching devices associated across the corresponding switches.

2.2.1. Analysis of DC-DC bidirectional converter

A storage system is a characteristic set-up to interface with the battery and SC to MG. The battery is a long-time ability of output power, a high-energy model by high density and slow response. SC is a high-power device with rapid response, high-energy efficiency, and exceptional power output abilities. In a power electronic system, a buck/boost converter is used. Both battery and SC are associated with low converter voltage. It is considered that D_{B1}, D_{B2}, D_{C1}, and D_{C2} are the duty cycles of $B1$, $B2$, $C1$, and $C2$. During the charging mode, the converter acts as a buck converter and power flow passes from the DC bus to storage units through the transfer function of DC voltage for SC and battery which is shown in (5). The boost converter functions during the discharging mode and the power transfers from SC or battery to DC bus with subsequent conversion ratio, as expressed in (6).

$$T_{VDC} = D_{B2} \text{ and } T_{VDC} = D_{C2} \tag{5}$$

$$T_{VDC} = \frac{1}{1-D_{B1}} \text{ and } T_{VDC} = \frac{1}{1-D_{C1}} \tag{6}$$

2.2.2. PI controller and SOC ESS

This converter operates in two modes: buck and boost. In the buck mode, the output voltage is decreased relative to input voltage while in boost mode, while output voltage is increased relative to the input voltage. Moreover, the boost mode obtains the final voltage which is higher than the supply end voltage. The significant parameter to estimate the battery state is SOC which is represented in (7). Where, I_{bat} represents the battery charging current and Q indicates battery capacity. Based on SOC, demand and battery power availability are to be charge-discharge. The battery's energy limitations are resolute based on SOC limits which are formulated in (8). The SOC_{min} and SOC_{max} indicates the minimum and maximum positions.

$$SOC = 100[1 + (\frac{I_{bat}dt}{Q}] \tag{7}$$

$$SOC_{min} \leq SOC \leq SOC_{max} \tag{8}$$

3. ADAPTIVE T-DISTRIBUTION DUNG BEETLE OPTIMIZATION (ADBO)

An effective EMS is developed by utilizing 2 different RES and 1 storage device. The PV module and wind turbine are the two different RES and a storage device is a battery utilized for storing the excess power from the wind and PV module. DBO [25] is a population-based algorithm that is primarily inspired by stealing, ball-rolling, foraging, dancing, and dung beetle reproduction behavior.

3.1. Ball-rolling dung beetle

Dung beetles navigate via celestial cues during a rolling procedure to maintain the rolling of the dung ball in a straight line. Hence, the ball-rolling dung beetle position is reorganized which is represented in (9) and (10). The t indicates the present number of iterations, $x_i(t)$ determines position data of ith dung beetle at t^{th} iteration, b denotes constant value, α represents natural coefficient, X^ω depicts the global worst position, and Δx indicates light intensity. Dung beetle's ball-rolling position is restructured and formulated in (11). Where $\theta \in [0, \pi]$ indicates the deflection angle.

$$x_i(t + 1) = x_i(t) + \alpha \times k \times x_i(t - 1) + b \times \Delta x \tag{10}$$

$$\Delta x = |x_i(t) - X^\omega| \tag{11}$$

$$x_i(t + 1) = x_i(t) + \tan(\theta)|x_i(t) - x_i(t - 1)| \tag{12}$$

3.2. Brood ball

Selecting an appropriate spawning site is essential for dung beetles to offer a safe atmosphere for their offspring. Therefore, a boundary selection model is used in DBO to pretend female dung beetles are expressed in (13). The X^* indicates the present local optimum position, Ub^* and Lb^* denotes the upper and lower bounds of the spawning area, $R = 1 - \frac{t}{T_{max}}$, T_{max} indicates the maximum number of iterations, Ub and Lb determines the upper and lower bounds of search space. A spawning area's boundary range is dynamically changed with values. Hence, the egg ball position also changes during an iteration procedure which is formulated in (14). $B_i(t)$ represents i^{th} sphere position at t^{th} iteration, b_1 and b_2 signify two independent random vectors.

$$\begin{aligned} Lb^* &= \max(X^* \times (1 - R), Lb) \\ Ub^* &= \min(X^* \times (1 - R), Ub) \end{aligned} \tag{13}$$

$$B_i(t + 1) = X^* + b_1 \times (B_i(t) - Lb^*) + b_2 \times (B_i(t) - Ub^*) \tag{14}$$

3.3. Small dung beetle

While the small beetles mature within the brood balls, they eventually emerge to search for food. Hence, it is required to find the optimal foraging area to guide them for searching food to achieve space exploration purposes. However, small dung beetle suffers from slow convergence speed. Therefore, an adaptive t-distribution is developed to balance exploitation and exploration which enhances the convergence speed during the dung beetles foraging stage. This technique equips DBO with an enhanced ability for global development through the initial iterations which is indicated in (15) and (16).

$$X_{new}^j = X_{best}^j + t(C_{iter}).X_{best}^j \tag{15}$$

$$C_{iter} = 1/\exp(-4 \times (t/M)^2) \tag{16}$$

Where, X_{new}^j denotes the position vector, X_{best}^j indicates a global best solution determined in the present iteration stage, C_{iter} represents the adaptive t-distribution parameter, $t(C_{iter})$ denotes a random number presented from adaptive t-distribution, and M presents a maximum number of iterations. This adaptive approach corresponds to the model's exploratory and developmental abilities which enhances its convergence rate and increases both its effectiveness and efficiency in solving optimization issues.

3.4. Thief dung beetle location update

Considering that the position of global optimum acts as the most appropriate target for theft, the updated position formula for thief dung beetles is formulated in (17). The $X_i(t)$ indicates the position of ith thief at t iteration, g represents a random vector that follows a normal distribution, D denotes dimensionality issues and S represents the constant value utilized in this approach. The ADBO provides an effective EMS via its adaptation of rolling behavior which mimics streamlined decision-making as well as resource allocation in complex systems and Figure 2 represents the flowchart for ADBO.

$$x_i(t + 1) = X^b + S \times g \times (|x_i(t) - X^*| + |X_i(t) - X^b|) \tag{17}$$

The process starts with initializing parameters and population while determining the fitness function for candidate solutions. The ADBO updates the position of the pushing dung beetle and determines whether a condition is satisfied. If the condition holds, the position is updated by employing a specific equation; else, it switches to an obstructed state and updates its position. The lower and upper bounds are used for constraining

the new position. Next, the t-distribution is used to refine its positions and then global and worst positions are updated if the convergence criteria are met. It is met, the algorithm stops processing; else, the process continues.
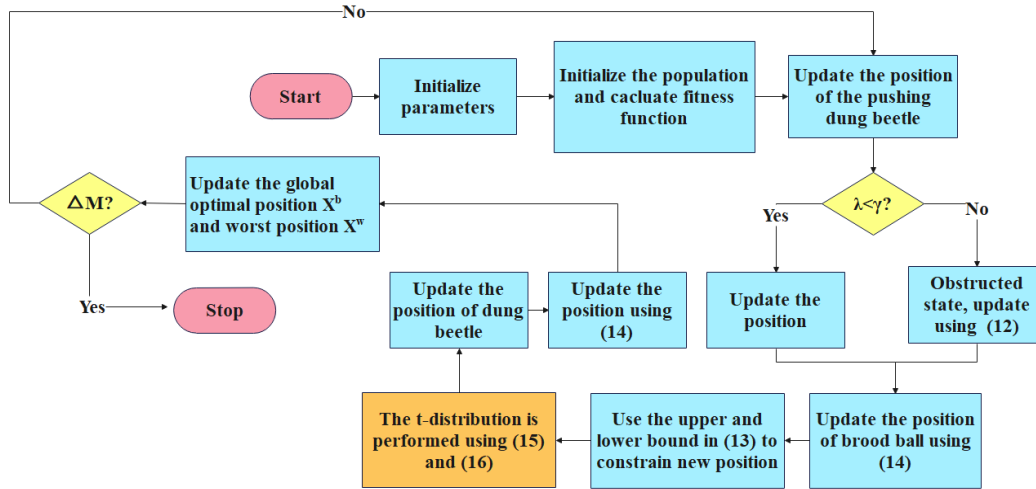
Figure 2. Flowchart for ADBO

3.5. Adaptive perturb and observe (AP&O)

This research utilizes AP&O for optimal MPPT in various weather conditions. This approach is applied to manage a duty-cycle perturbation step size which results in faster convergence tracking. A hypotenuse length of every triangle is computed according to Pythagoras theorem which is computed in (18). This theorem is determined by find the adaptive ΔD at i^{th} perturbation which is computed in (19).

$$hypotenuse\ length = \sqrt{V^2 + P^2} \tag{18}$$

$$\Delta D(i) = \Delta D_{min} + \sigma R(i) \tag{19}$$

Where, ΔD_{min} represents the lowest value included at every step, σ indicates scaling factor, $R(i)$ denotes the ratio among hypotenuse length for MPP triangle (L_{MPP}) hypotenuse length of OP triangle (L_{OP}) which is formulated in (20). V_M and P_M indicates PV voltage and maximum power point, V_{pv} and P_{pv} represents the voltage and power of the PV panel at the associated perturbation instant. Using AP&O in EMS enables dynamic adjustments of duty-cycle perturbation step sizes based on the present operating conditions which enhances efficiency and stability while varying loads and environmental factors.

$$R(i) = \frac{L_{MPP}}{L_{OP}} = \frac{\sqrt{V_M^2 + P_M^2}}{\sqrt{V_{pv}^2 + P_{pv}^2}} \tag{20}$$

4.   RESULTS AND DISCUSSION

This section represents the simulation results of the proposed ADBO-APO to establish the EMS effectively. To obtain the results, MATLAB R2020a is used with 64 GB RAM, a Windows 10 operating system, and an I5 Intel processor. The specification parameters of ADBO-APO are: a temperature of 35 °C, a base wind speed of 8 m/s, an initial SOC of 9%, a battery response time of 0.4 s, and an irradiation of 1000 $(\frac{W}{m^2})$.

4.1. Performance analysis

Figure 3 indicates a performance analysis of solar irradiation for the proposed ADBO-APO. The solar irradiation begins at 100 $(\frac{W}{m^2})$, increasing to a peak of around 950 $(\frac{W}{m^2})$ steadily at approximately 0.4 seconds, then briefly inclining and stabilizing nearby to 900 $(\frac{W}{m^2})$ before falling back to 100 $(\frac{W}{m^2})$ by 0.8 seconds, and at least drops to 0 $(\frac{W}{m^2})$ by 1 second. By analyzing these patterns, solar energy systems manage fluctuations and ensure a more stable and effective energy output.

Figure 4 depicts the performance analysis of wind speed for the ADBO-APO method. This graph shows the variation in wind speed over a 1-second interval. The speed of wind starts at around 13 m/s which remains constant till 0.3 seconds, then drops to 0 m/s and stays till 0.6 seconds. After 0.6 seconds, the speed of wind is increased rapidly to 15 m/s approximately and remains constant for the remaining interval. Figure 5 depicts the performance analysis of existing DBO's load demand, PV, wind, and battery without EMS. The load demand shows significant peaks around mid-day and afternoon hours. The PV power follows a similar pattern peaking during daylight hours. Figure 6 represents the proposed ADBO-APO's load demand, PV, wind, and battery with EMS. The EMS ensures a stable and balanced power supply by dynamically handling the sources which maintains a consistent load with minimal deviations.

Figure 7 represents the performance analysis of PV power. The blue line indicates the existing DBO approach while the orange line determines the proposed ADBO-APO approach. The proposed method shows a smoother and higher peak power generation which enhances the efficiency with better utilization of sunlight throughout the day.

Table 2 demonstrates a performance analysis of total harmonic distortion (THD). When compared to the existing methods like ant colony optimization-APO (ACO-APO), butterfly optimization algorithm-APO (BOA-APO), and DBO-APO, the proposed ADBO-APO achieves a better THD of 0.65%. Due to this, the proposed approach enhances the ability in varying conditions and optimizes the system more effectively.
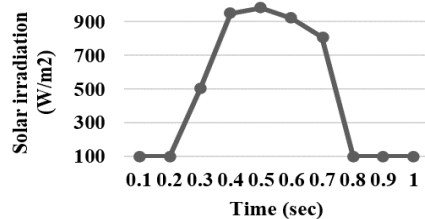

Figure 3. Performance of solar irradiation for the proposed approach
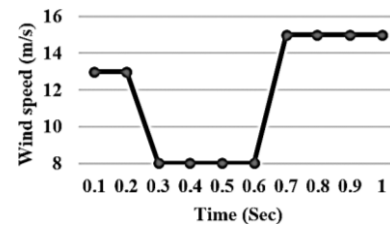

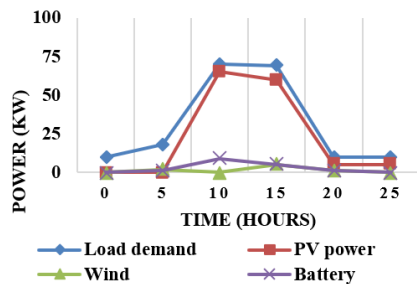Figure 4. Performance of wind speed for the proposed approach

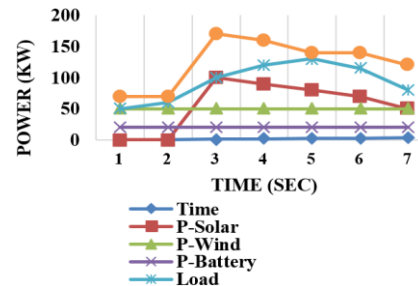Figure 5. Existing load demand, PV, wind, and battery without EMS

Figure 6. Proposed ADBO-APO's load demand, PV, wind, and battery with EMS
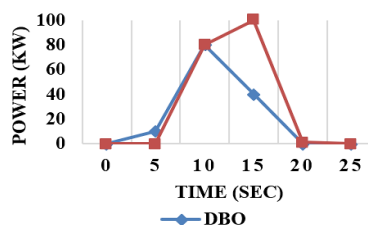

Figure 7. Performance analysis of PV power

Table 2. Performance analysis of THD

Methods	THD (%)
ACO-APO	4.12
BOA-APO	3.76
DBO-APO	2.43
Proposed ADBO-APO	0.65

4.2. Comparative analysis

Tables 3 and 4 indicate the comparative analysis of the proposed method with the Genetic algorithm and LFQOBL-SAO. Compared to the existing methods [18] and [19], the proposed ADBO-APO achieves better performance. Compared to [19], the proposed approach attains a superior average index of 1.2598×10^4 by enhancing the efficiency of EMS through optimal switching among battery, PV, and wind turbines.

Table 3. Comparative analysis of the proposed method with genetic algorithm

Conditions	Methods	Grid Purchase cost (Rs)	Battery degradation cost (Rs)
PV module – 1000 kW, 273.5 V	Genetic algorithm [18]	1.61×10^7	1.55×10^{12}
Battery rating- 500 Ah, 700 V Wind turbine – 1500 kW, 575 V	Proposed ADBO-APO	1.27×10^7	1.04×10^{12}

Table 4. Comparative analysis of proposed method with LFQOBL-SAO

Conditions	Methods	Index		
		Best	Average	Standard deviation
PV module – \$ 240 kW	LFQOBL-SAO [19]	1.5100×10^4	1.5274×10^4	1.2862×10^{-11}
Battery – 2.4 kWh	Proposed ADBO-APO	1.2423×10^4	1.2598×10^4	1.1768×10^{-11}
Wind turbine – \$ 1250 kW				

4.3. Discussion

The advantages of the proposed ADBO-APO method and the disadvantages of the existing methods are presented in this section. The disadvantage of existing methods is noted as follows: The [18] was trapped in local optima because of its dependence on the evolving solutions through a process of selection, mutation, and crossover. The result in [19] was based on historical data and predefined flight patterns and [21] faces struggles with the integration and coordination of multiple energy sources. The proposed ADBO-APO overcomes these existing method limitations. ADBO enhances the efficiency of EMS by ensuring optimal switching among battery and wind turbines. The APO increases the stability of power output from PV/wind/battery systems to adjust the DC-DC converter switching which ensures optimal power point tracking.

5. CONCLUSION

This research proposes ADBO-APO to establish an effective EMS by using three different sources PV, wind, and batteries. The ADBO-APO leverages its adaptive and cooperative strategies to optimize energy distribution and balancing which significantly increases overall reliability and effectiveness under dynamic conditions. The findings demonstrate that the proposed ADBO-APO not only enhances the system efficiency and reliability but also optimizes conversion and power management over different energy sources. The proposed ADBO-APO in relation to the existing method LFQOBL-SAO offers a superior average index of 1.2598×10^4. These outcomes support claims from previous research which represents that the proposed approach provides a significant enhancement in the EMS field. In the future, improved optimization will be considered with different controllers to enhance the model performance.

REFERENCES

[1]   M. M. Iqbal, S. Kumar, C. Lal, and C. Kumar, "Energy management system for a small-scale microgrid," *Journal of Electrical Systems and Information Technology*, vol. 9, no. 1, 2022, doi: 10.1186/s43067-022-00046-1.

[2]   G. Anusha, K. Arora, H. Sharma, S. P. Thota, G. P. Joshi, and W. Cho, "Control strategies of 15-level modified cascaded H-bridge MLI with solar PV and energy storage system," *Energy Reports*, vol. 12, pp. 2–26, Dec. 2024, doi: 10.1016/j.egyr.2024.06.003.

[3]   E. Hosseini *et al.*, "Optimal energy management system for grid-connected hybrid power plant and battery integrated into multilevel configuration," *Energy*, vol. 294, 2024, doi: 10.1016/j.energy.2024.130765.

[4]   O. Ceylan, M. Neshat, and S. Mirjalili, "Cascaded H-bridge multilevel inverters optimization using adaptive grey wolf optimizer with local search," *Electrical Engineering*, vol. 106, no. 2, pp. 1765–1779, 2024, doi: 10.1007/s00202-021-01441-z.

[5]   P. Horrillo-Quintero, P. García-Triviño, R. Sarrias-Mena, C. A. García-Vázquez, and L. M. Fernández-Ramírez, "Fault-tolerant control for a microgrid with PV systems and energy storage systems integrated into quasi-Z-source cascaded H-bridge multilevel inverter," *Electric Power Systems Research*, vol. 226, 2024, doi: 10.1016/j.epsr.2023.109938.

[6]   S. dos S. Bettoni, H. de O. Ramos, F. F. Matos, and V. F. Mendes, "Cascaded H-Bridge Multilevel Converter Applied to a Wind Energy Conversion System with Open-End Winding," *Wind*, vol. 3, no. 2, pp. 232–252, 2023, doi: 10.3390/wind3020014.

[7]   A. A. Al-Samawi and H. Trabelsi, "New Nine-Level Cascade Multilevel Inverter with a Minimum Number of Switches for PV Systems," *Energies*, vol. 15, no. 16, 2022, doi: 10.3390/en15165857.

[8]   F. Z. Khemili, O. Bouhali, M. Lefouili, L. Chaib, A. A. El-Fergany, and A. M. Agwa, "Design of Cascaded Multilevel Inverter and Enhanced MPPT Method for Large-Scale Photovoltaic System Integration," *Sustainability (Switzerland)*, vol. 15, no. 12, 2023, doi: 10.3390/su15129633.

[9]   K. R. Kumar, M. Venkatesan, and R. Saravanan, "A hybrid control topology for cascaded multilevel inverter with hybrid renewable energy generation subsystem," *Solar Energy*, vol. 242, pp. 323–334, 2022, doi: 10.1016/j.solener.2022.07.021.

[10] B. Gopinath, S. Suresh, G. Jayabaskaran, and M. Geetha, "Renewable energy resource integrated multilevel inverter using evolutionary algorithms," *Automatika*, vol. 65, no. 3, pp. 1061–1078, 2024, doi: 10.1080/00051144.2024.2329494.

[11] P. Horrillo-Quintero, P. García-Triviño, R. Sarrias-Mena, C. A. García-Vázquez, and L. M. Fernández-Ramírez, "Model predictive control of a microgrid with energy-stored quasi-Z-source cascaded H-bridge multilevel inverter and PV systems," *Applied Energy*, vol. 346, 2023, doi: 10.1016/j.apenergy.2023.121390.

[12] G. Liang *et al.*, "A Constrained Intersubmodule State-of-Charge Balancing Method for Battery Energy Storage Systems Based on the Cascaded H-Bridge Converter," *IEEE Transactions on Power Electronics*, vol. 37, no. 10, 2022, doi: 10.1109/TPEL.2022.3170062.

[13] A. O. Ali, A. M. Hamed, M. M. Abdelsalam, M. N. Sabry, and M. R. Elmarghany, "Energy management of photovoltaic-battery system connected with the grid," *Journal of Energy Storage*, vol. 55, 2022, doi: 10.1016/j.est.2022.105865.

[14] X. Fan, R. Zhao, J. He, H. Fan, Y. Xie, and T. Zhang, "Hybrid SVPWM Strategy of Cascade H-Bridge Multilevel Converter for Battery Energy Storage System," *IEEE Transactions on Power Electronics*, vol. 39, no. 1, pp. 626–635, 2024, doi: 10.1109/TPEL.2023.3302705.

[15] S. Jayaprakash, R. Balamurugan, S. Gopinath, T. Kokilavani, and S. Maheswaran, "3-Phase multi-inverter with cascaded H-bridge inverter designing and implementation for renewable system," *Sustainable Energy Technologies and Assessments*, vol. 52, 2022, doi: 10.1016/j.seta.2022.102088.

[16] A. Gupta, "Power quality evaluation of photovoltaic grid interfaced cascaded H-bridge nine-level multilevel inverter systems using D-STATCOM and UPQC," *Energy*, vol. 238, 2022, doi: 10.1016/j.energy.2021.121707.

[17] Z. Medghalchi and O. Taylan, "A novel hybrid optimization framework for sizing renewable energy systems integrated with energy storage systems with solar photovoltaics, wind, battery and electrolyzer-fuel cell," *Energy Conversion and Management*, vol. 294, 2023, doi: 10.1016/j.enconman.2023.117594.

[18] I. Wasiak *et al.*, "Innovative energy management system for low-voltage networks with distributed generation based on prosumers' active participation," *Applied Energy*, vol. 312, 2022, doi: 10.1016/j.apenergy.2022.118705.

[19] H. T. Dinh, K. haeng Lee, and D. Kim, "Supervised-learning-based hour-ahead demand response for a behavior-based home energy management system approximating MILP optimization," *Applied Energy*, vol. 321, 2022, doi: 10.1016/j.apenergy.2022.119382.

[20] V. V. Babu, J. Preetha Roselyn, and P. Sundaravadivel, "Multi-objective genetic algorithm based energy management system considering optimal utilization of grid and degradation of battery storage in microgrid," *Energy Reports*, vol. 9, pp. 5992–6005, 2023, doi: 10.1016/j.egyr.2023.05.067.

[21] A. A. Mas'ud *et al.*, "A Quasi oppositional smell agent optimization and its levy flight variant: A PV/Wind/battery system optimization application," *Applied Soft Computing*, vol. 147, 2023, doi: 10.1016/j.asoc.2023.110813.

[22] S. Boualem, O. Kraa, M. Benmeddour, M. Kermadi, M. Maamir, and H. Cherif, "Power management strategy based on Elman neural network for grid-connected photovoltaic-wind-battery hybrid system," *Computers and Electrical Engineering*, vol. 99, 2022, doi: 10.1016/j.compeleceng.2022.107823.

[23] M. Azaroual, N. T. Mbungu, M. Ouassaid, M. W. Siti, and M. Maaroufi, "Toward an intelligent community microgrid energy management system based on optimal control schemes," *International Journal of Energy Research*, vol. 46, no. 15, pp. 21234–21256, 2022, doi: 10.1002/er.8343.

[24] Z. Ullah *et al.*, "Implementation of various control methods for the efficient energy management in hybrid microgrid system," *Ain Shams Engineering Journal*, vol. 14, no. 5, 2023, doi: 10.1016/j.asej.2022.101961.

[25] J. Xue and B. Shen, "Dung beetle optimizer: a new meta-heuristic algorithm for global optimization," *Journal of Supercomputing*, vol. 79, no. 7, pp. 7305–7336, 2023, doi: 10.1007/s11227-022-04959-6.

BIOGRAPHIES OF AUTHORS
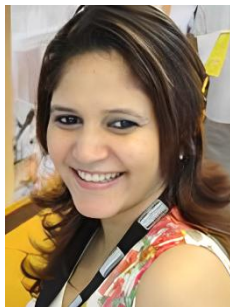
Shweta Sengar is a dedicated research scholar pursuing a Ph.D. in Engineering. With a strong academic foundation, including an M.Tech. in Energy Management and a B.E. in Instrumentation and Control, her research focuses on load forecasting and hybrid machine learning algorithms. She has contributed significantly to the field with her publications and is actively engaged in academic teaching and mentoring. She can be contacted at email: shwetasengar17@gmail.com.

Aniket Kumar is currently working as an associate professor and Director in the School of Electronics, Electrical and Mechanical Engineering, SIET, Meerut. He joined the institute in the year 2015. He is actively involved in various academic and administrative responsibilities at the University level and School levels. Presently, he is guiding students at the Doctorate level. He has also received a Pillars of The Nation Award from the Institute for Social Reforms and Higher Education Charitable Trust, Registered with NITI Aayog, GOI., and a teacher innovation award from Sri Aurobindo Society, for Sustainable Efforts Towards Promoting Joyful and Experiential Teaching. His research interest includes digital systems design, signal processing, and Vedic mathematics. He has more than twenty-one patents and Eighty-Five research publications six books to his credit in national and international Journals/conferences of repute and four books as author and editor. He can be contacted at email: aniket.kumar@shobhituniversity.ac.in.